

## Spectroscopic Studies on Ligand–Enzyme Interactions: Complexation of $\alpha$ -Chymotrypsin with 4',6-Diamidino-2-phenylindole (DAPI)

Debapriya Banerjee, Sachin Kumar Srivastava, and Samir Kumar Pal\*

Unit for Nano Science & Technology, Department of Chemical, Biological & Macromolecular Sciences, S. N. Bose National Centre for Basic Sciences, Block JD, Sector III, Salt Lake, Kolkata 700 098, India

Received: October 2, 2007; In Final Form: November 23, 2007

In the present study, the interaction of two structurally related proteolytic enzymes trypsin and  $\alpha$ -chymotrypsin (CHT) with 4',6-Diamidino-2-phenylindole (DAPI) has been addressed. The binding of DAPI to CHT has been characterized by steady-state and picosecond time-resolved spectroscopic techniques. Enzymatic activity of CHT and simultaneous binding of the well-known inhibitor proflavin (PF) in the presence of DAPI clearly rule out the possibility of DAPI binding at the catalytic site of the enzyme. The spectral overlap between the emission of DAPI and absorption of PF offers the opportunity to explore the binding site of DAPI using Förster resonance energy transfer (FRET). FRET studies between DAPI and PF indicate that DAPI is bound to CHT with its transition dipole nearly perpendicular to that of PF. Competitive binding of DAPI with another fluorescent probe 2,6-*p*-toluidinonaphthalene sulfonate (TNS), having a well-defined binding site, indicates that DAPI and TNS bind at the same hydrophobic site of the enzyme CHT. The difference in the interactions of two well-studied, structurally similar enzymes with the same molecule may find its application in the design of specific substrate mimics or inhibitors of the enzymes.

### Introduction

The correlation between structure and function of biomolecules is a long-standing problem in biology. Structurally similar biomolecules exhibit differences in function,<sup>1</sup> whereas molecules, which are structurally dissimilar, show similarities of function.<sup>2</sup> The correlation between structure and function can be attributed to different molecular recognition by substrates/ligands of biomolecules,<sup>3,4</sup> giving rise to the concept of substrate/ligand specificity. Since substrate specificity of biomolecules is crucial for almost every biological function, the exploration of the origin of substrate specificity has due importance for the design of molecules that could mimic the naturally occurring substrates or inhibit the activity of the concerned biomolecule. The diversity of substrate specificity within a single structural motif is well-illustrated by the trypsin family of serine proteases. The representative enzymes trypsin and chymotrypsin are hydrolytic in nature having similar structure but very different substrate specificities: trypsin hydrolyzes peptides with arginine or lysine residues, while chymotrypsin prefers peptides with large hydrophobic residues.<sup>5</sup> The difference in substrate specificities of trypsin and chymotrypsin appears to result from simple structural alterations of the S1 binding pocket (active site) of these proteases: Aspartate (Asp189) at the bottom of the S1 binding pocket of trypsin accounts for its specificity for positively charged residues; the analogous residue in chymotrypsin is serine (Ser189), which creates a more hydrophobic S1 binding pocket. However, site-directed mutagenesis studies have shown that mutation of the residues of the substrate-binding pocket of trypsin to the analogous residues of chymotrypsin does not convert trypsin into a protease with chymotrypsin-like specificity.<sup>5</sup> It has been shown that chymotrypsin-like

substrate specificity is attained when two surface loops of trypsin are changed to the analogous residues of chymotrypsin, in conjunction with the changes in the S1 binding site.<sup>6</sup> The exploration of the effect of the modest structural differences that characterize these two serine proteases on their interactions with ligands is worthwhile for the design of appropriate substrate mimics and inhibitors of these enzymes.

The discovery of the effectiveness of benzamide as an anti-trypsin agent by Mares Guia and Shaw<sup>7</sup> has triggered research in the development of synthetic inhibitors of serine proteases.<sup>8</sup> The three-dimensional structures of trypsin with the pseudosubstrate benzamidine<sup>9,10</sup> suggest that the carboxylate group of Asp189, at the base of the trypsin binding pocket, is largely responsible for the specificity in binding of the positively charged amino acid side chains to the enzyme. The molecule 4',6-Diamidino-2-phenylindole (DAPI) contains two benzamidine groups and is an inhibitor of trypsin. X-ray crystallographic studies show that DAPI binds to the active site of trypsin.<sup>11</sup> The binding of dicationic DAPI to trypsin is in accordance with the specificity of trypsin for basic residues. On the other hand, studies on the interaction of DAPI with biomimetic micelles (to be published elsewhere) have revealed that the interaction of DAPI with micelles is dominated by charge interactions, rather than hydrophobic interactions. Thus, the molecular recognition of  $\alpha$ -chymotrypsin (CHT) by the trypsin inhibitor and fluorescent probe DAPI is an ideal tool to investigate the correlation between structure, hydrophobicity and molecular recognition of these structurally related enzymes.

In this report, steady-state, picosecond time-resolved fluorescence and polarization-gated anisotropy have been used to study the interaction of DAPI with CHT. The position and the binding geometry of DAPI to CHT have been investigated using Förster resonance energy transfer (FRET) to a well-known inhibitor chromophore proflavin (PF) in the active site of the

\* Corresponding author. E-mail: skpal@bose.res.in. Fax: 91 33 2335 3477.

enzyme. The efficacy of PF and DAPI as donor acceptor pair in FRET has been confirmed through a control study in SDS micelles. The enzymatic activity of the DAPI–CHT complex has also been studied. To ascertain the binding site of DAPI in CHT, the change in fluorescence of the DAPI–CHT complex in solutions with different pH values and competitive binding studies with another CHT binding probe 2,6-*p*-toluidinonaphthalene sulfonate (TNS) have been studied. Our studies on the difference in the interaction of two well-studied structurally similar enzymes with the same probe may find application in the design of specific substrate mimics or inhibitors of the enzymes.

## Materials and Methods

Bovine pancreatic  $\alpha$ -chymotrypsin (CHT), Ala–Ala–Phe–7-amido-4-methylcoumarin (AMC), 2,6-*p*-toluidinonaphthalene sulfonate (TNS) and proflavin (PF) are from Sigma. Phosphate buffer is from Merck. 4',6-Diamidino-2-phenylindole (DAPI) is from Molecular Probes. Sodium dodecyl sulfate (SDS) is from Fluka. The solutions are prepared in 100 mM phosphate buffer (pH 7.0) using water from the Millipore system. The probe–protein solutions are prepared by adding a requisite amount of probe to the protein solution and stirring for 1 h. To ensure complete complexation of probe with the protein, the probe concentration is kept much less (1  $\mu$ M) than the protein concentration (100  $\mu$ M). For the energy transfer studies, the concentration of the donor (DAPI) is kept much less and the concentration of the acceptor (PF) is kept equal to the macromolecular (protein/micelles) concentration. This eliminates the possibility of homomolecular energy transfer between donors and ensures that, for every donor attached to a macromolecule, there is an acceptor bound to the same macromolecule. In the enzymatic activity studies, [DAPI] = [CHT] = 1  $\mu$ M, and the concentration of substrate AMC is 100  $\mu$ M. The details of the measurement of enzymatic activity are reported elsewhere.<sup>12</sup> For competitive binding studies, DAPI is progressively added to the TNS–CHT complex ([TNS]/[CHT] = 1:100), until the final concentration of DAPI is equal to that of CHT.

Steady-state absorption and emission are measured with Shimadzu UV-2450 spectrophotometer and Jobin Yvon Fluoromax-3 fluorimeter, respectively. An excitation wavelength of 375 nm is used to excite both DAPI and TNS molecules in the steady-state fluorescence studies. The excitation spectrum of DAPI in CHT is constructed by monitoring the emission at 457 nm (the peak of DAPI emission in CHT). Fluorescence transients are measured by using a spectrophotometer from Edinburgh Instrument (LifeSpec-ps), U.K. (an excitation wavelength of 375 nm is used for both DAPI and TNS, and the instrument response function (IRF) is 80 ps). The observed fluorescence transients are fitted by using a nonlinear least-squares fitting procedure to a function  $X(t) = \int_0^t E(t') R(t-t') dt'$  comprised of convolution of the IRF  $E(t)$  with a sum of exponentials  $R(t) = A + \sum_{i=1}^N B_i e^{-t/\tau_i}$  with pre-exponential factors ( $B_i$ ), characteristic lifetimes ( $\tau_i$ ) and a background ( $A$ ). Relative concentration in a multiexponential decay is finally expressed as  $c_n = [B_n / (\sum_{i=1}^N B_i)] \times 100$ . The quality of the curve fitting is evaluated from reduced chi-square and residual data. In order to estimate the Förster resonance energy transfer efficiency of the donor (DAPI) to the acceptor (PF) and hence to determine the distances between donor–acceptor pairs, we have followed the methodology described in chapter 13 of reference 13. The Förster distance ( $R_0$ ) is given by

$$R_0 = 0.211[\kappa^2 n^{-4} Q_D J(\lambda)]^{1/6} \quad (\text{in } \text{Å}) \quad (1)$$

where  $\kappa^2$  is a factor describing the relative orientation in space of the transition dipoles of the donor and acceptor. The value of  $\kappa^2$  is to be taken as 0.667 for random orientation. The refractive index ( $n$ ) of the medium is assumed to be 1.5.  $Q_D$ , the quantum yield of the donor in the absence of acceptor is measured to be 0.45 and 0.24 in SDS micelles and CHT, respectively.  $J(\lambda)$ , the overlap integral, which expresses the degree of spectral overlap between the donor emission and the acceptor absorption, is given by

$$J(\lambda) = \frac{\int_0^\infty F_D(\lambda) \epsilon(\lambda) \lambda^4 d\lambda}{\int_0^\infty F_D(\lambda) d\lambda} \quad (2)$$

where  $F_D(\lambda)$  is the fluorescence intensity of the donor in the wavelength range of  $\lambda$  to  $\lambda + d\lambda$  and is dimensionless.  $\epsilon(\lambda)$  is the extinction coefficient (in  $\text{M}^{-1} \text{cm}^{-1}$ ) of the acceptor at  $\lambda$ . If  $\lambda$  is in nm, then  $J(\lambda)$  is in units of  $\text{M}^{-1} \text{cm}^{-1} \text{nm}^4$ . Once the value of  $R_0$  is known, the donor–acceptor distance ( $r$ ) can easily be calculated using the formula

$$r^6 = [R_0^6 (1 - E)]/E \quad (3)$$

Here,  $E$  is the efficiency of energy transfer. The efficiency ( $E$ ) is calculated from the lifetimes of the donor in the absence and presence of acceptors ( $\tau_D$  and  $\tau_{DA}$ ).

$$E = 1 - (\tau_{DA}/\tau_D) \quad (4)$$

For anisotropy ( $r(t)$ ) measurements, emission polarization is adjusted to be parallel or perpendicular to that of the excitation and anisotropy is defined as

$$r(t) = \frac{[I_{\text{para}} - G \times I_{\text{perp}}]}{[I_{\text{para}} + 2 \times G \times I_{\text{perp}}]} \quad (5)$$

$G$ , the grating factor, is determined following the long-time tail matching technique.<sup>14</sup>

## Results and Discussion

Figure 1a shows the excitation and emission spectra of DAPI bound to  $\alpha$ -chymotrypsin (CHT). It is to be noted that, due to the huge absorption tail of CHT (present in high concentration in solution), the exact nature of the peak of DAPI bound to CHT is not discernible from the absorption spectra. The excitation spectrum is, therefore, reported here for the clarity of presentation. The excitation spectrum shows a peak at 356 nm corresponding to maximum absorption. The absorption peak of DAPI in CHT is red shifted compared to that of DAPI in buffer and is similar to the absorption peak of DAPI in DNA.<sup>15</sup> The emission spectrum of the DAPI–CHT complex shows a blue shift compared to that in buffer and a concomitant increase in fluorescence intensity. The steady-state results thus indicate interaction of DAPI with the protein. Figure 1b shows the temporal decay of fluorescence of DAPI in CHT. The decay has been fitted with time constants of 130 ps (75%), 1.0 ns (12%) and 3.0 ns (13%). The 130 ps component is similar to that obtained when the probe is in buffer.<sup>16,17</sup> In buffer, this 130 ps component represents the solvent-assisted intramolecular proton transfer process,<sup>16</sup> from the amidino to the indole moiety of DAPI.<sup>18</sup> The significant bulk-like component in the fluorescence transients is not due to the population of the probe in bulk water, as the temporal anisotropy (see below) of the probe in CHT stands against the presence of free type probe in the

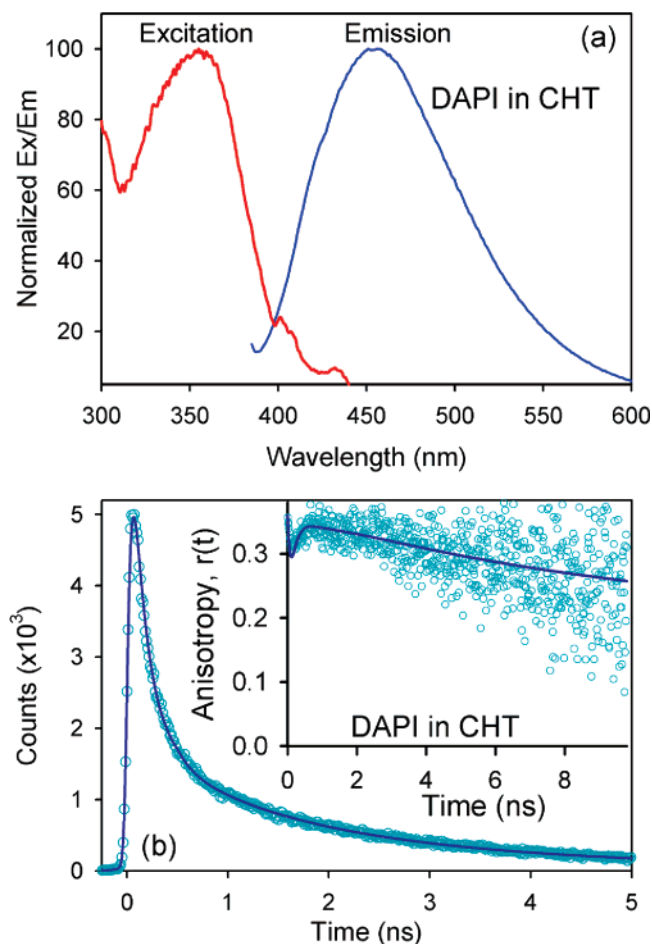


**Figure 1.** Absorption, emission (a), temporal decay of fluorescence (b), and anisotropy (inset b) of DAPI ( $1 \mu\text{M}$ ) in CHT ( $100 \mu\text{M}$ ).

DAPI–CHT complex. Therefore, the presence of a 130 ps component suggests that, in the CHT binding mode, the intramolecular proton transfer process in DAPI is still operative. A recent study<sup>15</sup> on the interaction of DAPI with DNA duplexes of various sequences has revealed that the retention of this fast component is possible in restricted environments in a binding geometry where the amidinoindole moiety of DAPI is solvent exposed. The longer components in the fluorescence decay are associated with the lifetime of the probe in the hydrophobic environment. Similar long components are observed in DAPI–DNA complexes.<sup>15</sup> The inset of Figure 1b shows the temporal decay of fluorescence anisotropy of the DAPI–CHT complex. The fluorescence anisotropy shows dip and rise in our experimental window. This type of anisotropy decay occurs in a system where there is a juxtaposition of very fast and slow motions of the excited dipole of the fluorophore.<sup>19,20</sup> The decay has been fitted with time constants of 500 ps (16%) and 11 ns (84%) associated with the rotational motions of the enzyme molecule. The faster component of 500 ps is associated with the faster rotation of the solvent exposed group of DAPI molecule, and the slow component stands for the slower rotation of the protein-bound part.

To explore whether DAPI binds in the S1 pocket as an inhibitor as it does in trypsin, the enzymatic activity of the DAPI–CHT complex is compared to that of CHT. Figure 2 shows the enzymatic activity of CHT and the DAPI–CHT complex in a 900 s time window. The initial linear rise parts are essentially similar for DAPI and DAPI–CHT complexes. The velocity of the reaction for the DAPI–CHT complex is 31 nM/s, which falls within the limit of experimental error (3 nM/

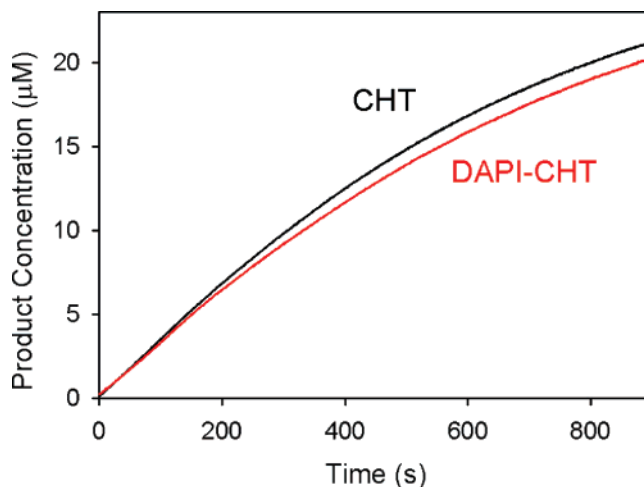


**Figure 2.** Enzymatic activity of the DAPI–CHT complex compared to that of CHT.

s) when compared with that of the native CHT (34 nM/s). It is to be noted that the velocity of the reaction varies substantially for protein and protein–inhibitor complexes. The observation clearly suggests that DAPI bound to CHT does not act as an inhibitor and hence does not bind in the active site (S1 site) of CHT. Addition of the well-established inhibitor proflavin (PF) to the DAPI–CHT complex shows that both DAPI and PF simultaneously bind CHT under the experimental conditions (discussed later). The observation further confirms the fact that DAPI does not bind in the active site of the molecule. Simultaneous binding of PF and DAPI to CHT offers a unique opportunity of using Förster resonance energy transfer (FRET) studies between the protein-bound probes. The FRET technique gives an accurate distance between two fluorescent probes, one of which acts as a donor and the other an acceptor. In our study, DAPI is the fluorescence donor and PF is the acceptor. The binding of PF in the active site of CHT is well-documented in the literature.<sup>21</sup> For DAPI and PF bound to CHT, Figure 3a shows the spectral overlap between the absorption spectrum of PF and emission of DAPI bound to CHT. There is appreciable spectral overlap, indicating that these two probes can serve as a good donor–acceptor pair in CHT. There is quenching of fluorescence intensity (Figure 3b) in the DAPI–PF–CHT complex relative to that of DAPI–CHT, reflecting energy transfer from DAPI to PF. The binding of PF to CHT in the PF–DAPI–CHT complex under the experimental conditions is given by the long fluorescence lifetime (inset of Figure 3c) and increased fluorescence intensity (Figure 3b) of the PF–CHT complex. However, the temporal fluorescence decays (Figure 3c) of DAPI in DAPI–CHT and DAPI–PF–CHT complexes show very little difference between the observed lifetimes, indicating very inefficient dipole–dipole coupling. The observation is also consistent with the reabsorption of donor emission by the acceptor PF, as evidenced in the steady-state emission spectra (Figure 3b).

The negligible energy transfer between DAPI and PF bound to CHT can have the following interpretations: (i) DAPI and PF are bound in the active site of CHT with unfavorable orientations of their transition dipoles. (ii) DAPI and PF are separated by a distance larger than the Förster distance ( $R_0$ ) with favorable orientations of transition dipoles. (iii) DAPI and PF are bound at a distance smaller than  $R_0$ , with unfavorable orientations of their transition dipoles. Let us examine the conditions one by one. The enzymatic activity of CHT in the presence of DAPI is similar to that of the native enzyme. This

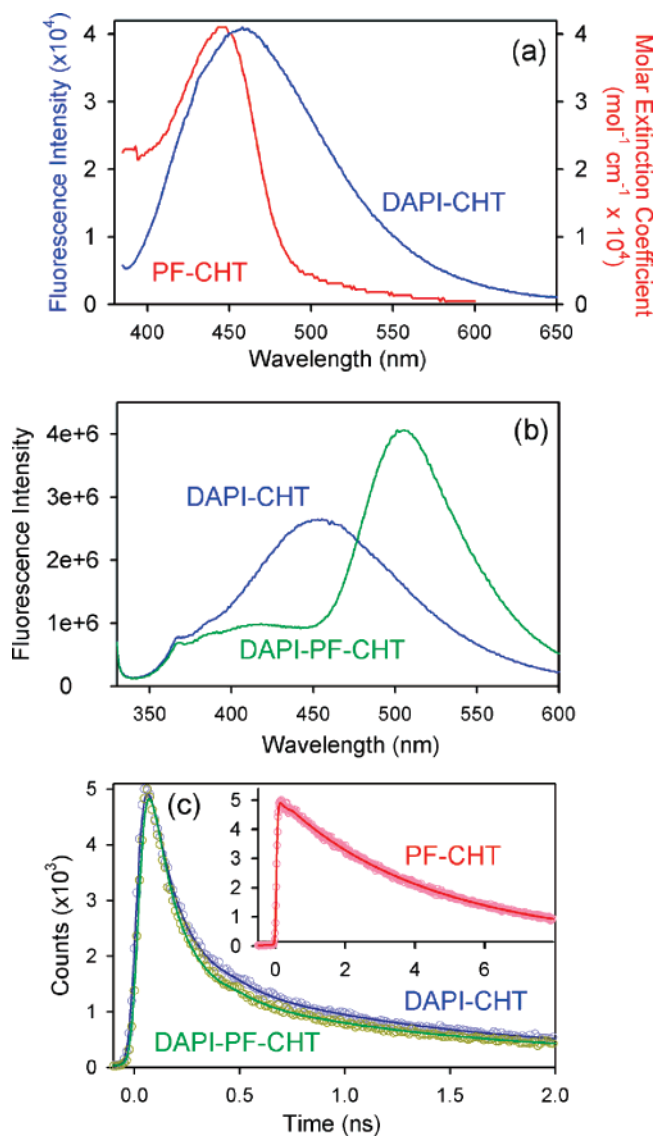


**Figure 3.** (a) Spectral overlap of DAPI and PF in 100  $\mu\text{M}$  CHT. The emission spectra (b) and the temporal decay (c) of DAPI (1  $\mu\text{M}$ ) and DAPI–PF ([PF] = 100  $\mu\text{M}$ ) in 100  $\mu\text{M}$  CHT.

suggests that DAPI is not inhibiting the enzymatic activity and hence is less likely bound in the active site. Also, had both DAPI and PF bound in the active site, there would have been a quenching of DAPI fluorescence due to Dexter resonance transfer.<sup>22,23</sup> Therefore, the possibility of PF and DAPI simultaneously occupying the active site of CHT is ruled out. The result is in agreement with the behavior of DAPI in hydrophobic environments. It is known that the interaction of DAPI with hydrophobic residues is dominated by favorable electrostatic interactions. The replacement of negatively charged Asp189 in trypsin (where DAPI binds at active site<sup>11</sup>) to Ser189 in CHT creates a more hydrophobic active site. The change in the polarity of the active site of CHT compared to trypsin and the associated structural changes thus accounts for the different interactions of trypsin and CHT with DAPI. The calculated value of  $R_0$  (considering random orientation of dipoles, i.e., a  $\kappa^2$  value of 0.66) for DAPI and PF in CHT is 3.76 nm, which is less than the distance between the active site and any point within or at the surface of CHT. The observation indicates that both the fluorophores are not bound to CHT at a distance greater than  $R_0$ , with favorable orientations of their transition dipoles. The absence of energy transfer, therefore, suggests that DAPI

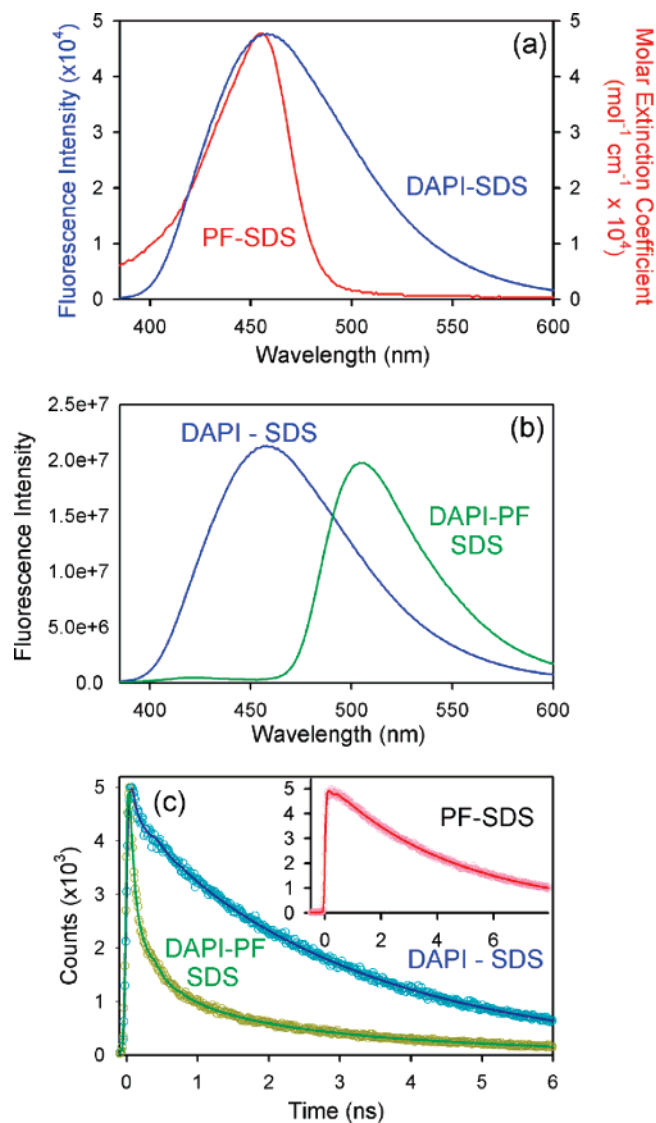


**Figure 4.** (a) Spectral overlap of DAPI and PF in SDS micelles (200  $\mu\text{M}$  micellar concentration). The emission spectra (b) and the temporal decay (c) of DAPI (1  $\mu\text{M}$ ) and DAPI–PF ([PF] = 200  $\mu\text{M}$ ) in 20 mM SDS.

and PF are being bound to CHT with perpendicular or nearly perpendicular orientation of their respective transition dipoles.

To further ensure that the absence of FRET between DAPI and PF bound to CHT is indeed due to unfavorable orientations of their transition dipoles, and also to check the suitability of DAPI–PF as a donor–acceptor pair, FRET between DAPI and PF is studied in SDS micelles. Both DAPI and PF bind at the interface of SDS micelles, having a random relative orientation of their transition dipoles. The SDS micelles are chosen because not only do they allow random orientations of their transition dipoles of the bound ligands but they also offer a close similarity of the size of the CHT molecules. Figure 4a shows significant spectral overlap between the emission spectrum of DAPI (donor) and the absorption spectrum of PF (acceptor) in SDS micelles. The binding of PF to SDS has been indicated by a longer lifetime of PF in the PF–DAPI–SDS complex (inset of Figure 4c). The energy transfer takes place from the donor to the acceptor, as indicated by the quenching of fluorescence intensity (Figure 4b) as well as the faster decay (Figure 4c) of the donor in the donor–acceptor complexes in micelles compared to that of the donor itself in the micelles. The results prove beyond a doubt that DAPI and PF is an effective pair for FRET. The

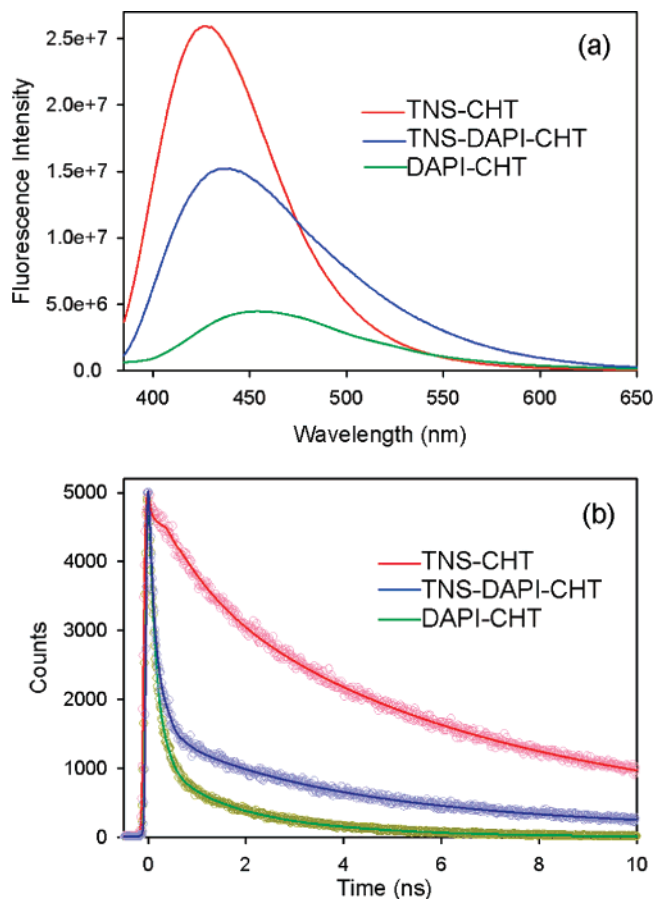


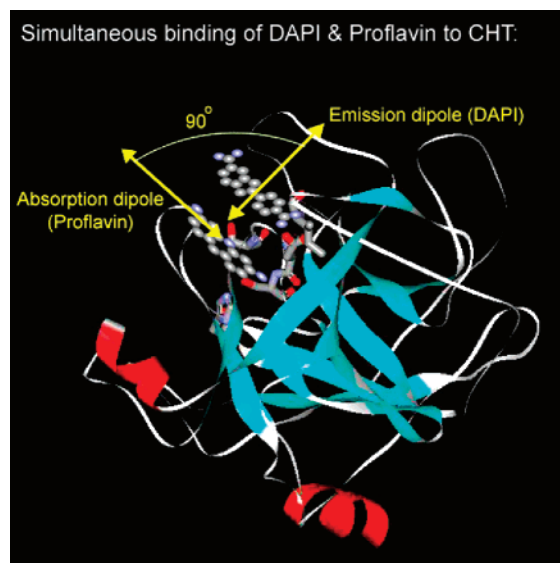
**Figure 5.** (a) Fluorescence spectra and (b) the temporal decay of fluorescence of TNS-CHT, TNS-DAPI-CHT and DAPI-CHT complexes. [TNS] = 2  $\mu$ M, [CHT] = 100  $\mu$ M and [DAPI] = 100  $\mu$ M.

distance between the donor and the acceptor has been calculated to be 3.32 nm, by using an  $R_0$  value of 3.87 nm. The observation is consistent with the binding of the donor and acceptor across the chords in the spherical SDS micelle (4 nm diameter<sup>24</sup>).

The studies of the enzymatic activity of the DAPI-CHT complex along with FRET studies in DAPI-PF-CHT complexes indicate that DAPI binds to CHT at some site other than the catalytic site. In addition to the catalytic binding site, two other sites in CHT, capable of binding ionic hydrophobic dye, are reported in the literature. The first one is the hydrophobic binding site proposed by Smith and Hansch,<sup>25</sup> which is known to bind the hydrophobic dye TNS,<sup>26</sup> and the other is the 1-anilinonaphthalene-8-sulfonate (ANS) binding site reported by Johnson et al.<sup>27</sup> The differences in the nature of the binding sites of TNS and ANS are reflected in the pH dependent fluorescence spectrum of TNS-CHT and ANS-CHT complexes. The fluorescence of the TNS-CHT complex shows a 15 nm red shift and an increase in fluorescence intensity as the pH of the medium is raised from 2.5 to 7.8.<sup>26</sup> On the other hand, the fluorescence spectra of ANS-CHT complexes show a red shift but a concomitant decrease in fluorescence intensity over the same pH range,<sup>27</sup> indicating the difference in the nature of binding sites of these two dyes. The fluorescence spectrum of DAPI-CHT shows a 20 nm red shift along with an increase in fluorescence intensity at high pH and is similar to the fluorescence behavior of the TNS-CHT complex.

In order to confirm the exact location of DAPI in CHT, competitive binding studies between DAPI and TNS are performed. TNS gives a fluorescence maximum at 427 nm, whereas DAPI shows an emission peak around 457 nm.

### SCHEME 1: Simultaneous Binding of DAPI (Donor) and PF (Acceptor) in CHT<sup>a</sup>



<sup>a</sup> From FRET studies, the relative orientation between the transition dipoles of the donor and acceptor is found to be nearly perpendicular. The molecular structure of CHT (2CHA) is downloaded from the Protein Data Bank and processed with the program Web Lab Viewer Lite.

However, the increase in fluorescence intensity of TNS in CHT ( $Q_D = 0.6$ ) is much more than that of DAPI ( $Q_D = 0.24$ ). Figure 5a shows the fluorescence spectrum of TNS-CHT and TNS-DAPI-CHT complexes. The quenching of fluorescence of TNS in TNS-DAPI-CHT indicates that TNS is being expelled out from the protein on addition of DAPI. Also, TNS in CHT shows a 9 ns lifetime, which is much longer than the longest lifetime component of DAPI in CHT (3 ns). Thus, this long component associated with the relaxation of TNS fluorescence in CHT can be monitored to characterize the binding of TNS to CHT. In this regard, it is to be noted that both TNS and DAPI absorb the 375 nm light used as our excitation source. This might raise the complication that the reported fluorescence is actually the average of the emission coming from the two fluorophores. However, the comparison of the emission spectrum of TNS-DAPI-CHT and DAPI-CHT (having the same concentration of DAPI as in the TNS-DAPI-CHT complex) shows that, at 410 nm, the fluorescence of TNS is 9 times more than that of DAPI. This ensures that, at 410 nm, the decay of fluorescence essentially reports the relaxation of the excited TNS molecules, with minimum interference from DAPI. The temporal decays of fluorescence in TNS-CHT and TNS-DAPI-CHT complexes at 410 nm are shown in Figure 5b. The fluorescence of DAPI-CHT having the same concentration of DAPI is also shown in Figure 5a for comparison. Analyses of the decays show that the 9 ns lifetime characteristic of the TNS-CHT complex decreases from 50 to 18% in the TNS-DAPI-CHT complex. This gives a clear indication that TNS is expelled on the addition of DAPI. In other words, DAPI competes for the binding site of TNS.

It is interesting to observe that, although the binding of TNS to CHT affects the enzymatic activity, the binding of DAPI in the same site leaves the enzymatic activity unaltered. The apparent anomaly in the behavior of these two dyes binding in the same site can be easily resolved if one considers the correlation between the ligand binding in this hydrophobic site<sup>25</sup> and the mechanism of enzyme inhibition.<sup>28</sup> The anionic TNS

binds in the hydrophobic environment of the isoleucine (Ile16) and Asp194 ion pair and through electrostatic repulsion displaces the Asp194 side chain in such a way that it blocks and inactivates the Ser195 and His57 active site. However, the cationic DAPI may form an alternate ion pair with Asp194 and hence does not effectively displace the Asp194, a phenomenon that is crucial for enzyme deactivation. To estimate the binding geometry of DAPI in the TNS-binding site, we use the result of energy transfer in the PF–DAPI–CHT complex. Estimating that the centers of the active site and the DAPI binding site are 1.2 nm apart, the value of the orientation factor  $\kappa^2$  is calculated to be close to zero. This indicates a perpendicular geometry of the PF and DAPI transition dipoles when PF and DAPI bind at the active site and TNS binding site, respectively, in CHT (Scheme 1).

### Conclusion

In the present study, the effect of structural modifications in different interactions of two structurally related proteolytic enzymes, trypsin and CHT, with DAPI has been addressed. Steady-state, picosecond time-resolved fluorescence and polarization-gated anisotropy have been used to characterize the binding of DAPI to CHT. The retention of enzymatic activity of CHT in the DAPI–CHT complex as well as the simultaneous binding of the potent inhibitor PF and DAPI to CHT rules out the possibility of DAPI binding at the active site. Competitive binding studies with TNS in CHT show that TNS is expelled out from the enzyme with the progressive addition of DAPI, indicating that DAPI binds at the TNS binding site. FRET studies between DAPI and PF indicate that DAPI is bound at the TNS binding site of CHT in such a geometry that the transition dipoles of PF and DAPI are nearly perpendicular to each other (Scheme 1). The difference in interaction of the two proteolytic enzymes with DAPI can be exploited for the design of specific substrate mimics or inhibitors of these enzymes.

**Acknowledgment.** D.B. thanks CSIR India for a fellowship. We thank DST for a financial grant (SR/FTP/PS-05/2004).

### References and Notes

(1) Yoon, S.; Jones, B. C.; Logsdon, N. J.; Walter, M. R. *Structure* **2005**, *13*, 551–564.

- (2) Kisselev, L. *Structure* **2002**, *10*, 8–9.
- (3) Erickson, J. A.; Jalaie, M.; Robertson, D. H.; Lewis, R. A.; Vieth, M. J. *Med. Chem.* **2004**, *47*, 45–55.
- (4) Tyndall, J. D. A.; Fairlie, D. P. *J. Mol. Recognit.* **1999**, *12*, 363–370.
- (5) Graf, L.; Jancso, A.; Szilagyi, L.; Hegyi, G.; Pinter, K.; Naray-Szabo, G.; Hepp, J.; Medzihradsky, K.; Rutter, W. J. *Proc. Natl. Acad. Sci. U.S.A.* **1988**, *85*, 4961–4965.
- (6) Hedstrom, L.; Szilagyi, L.; Rutter, W. J. *Science* **1992**, *255*, 1249–1253.
- (7) Mares-Guia, M.; Shaw, E. *J. Biol. Chem.* **1965**, *240*, 1579–1585.
- (8) Han, Q.; Dominguez, C.; Stouten, P. F. W.; Park, J. M.; Duffy, D. E.; Glemmo, R. A., Jr.; Rossi, K. A.; Alexander, R. S.; Smallwood, A. M.; Wong, P. C.; Wright, M. M.; Luettgen, J. M.; Knabb, R. M.; Wexler, R. R. *J. Med. Chem.* **2000**, *43*, 4398–4415.
- (9) Bode, W.; Schwager, P. *J. Mol. Biol.* **1975**, *98*, 693–717.
- (10) Huber, R.; Bode, W. *Acc. Chem. Res.* **1978**, *11*, 114–122.
- (11) Casale, E.; Collyer, C.; Ascenzi, P.; Balliano, G.; Milla, P.; Viola, F.; Fasano, M.; Menegatti, E.; Bolognesi, M. *Biophys. Chem.* **1995**, *54*, 75–81.
- (12) Biswas, R.; Pal, S. K. *Chem. Phys. Lett.* **2004**, *387*, 221–226.
- (13) Lakowicz, J. R. *Principles of fluorescence spectroscopy*; Kluwer Academic/Plenum: New York, 1999.
- (14) O'Connor, D. V.; Philips, D. *Time correlated single photon counting*; Academic Press: London, 1984.
- (15) Banerjee, D.; Pal, S. K. *J. Phys. Chem. B* (in press).
- (16) Barcellona, M. L.; Gratton, E. *Biophys. Chem.* **1991**, *40*, 223–229.
- (17) Barcellona, M. L.; Cardiel, G.; Gratton, E. *Biochem. Biophys. Res. Commun.* **1990**, *170*, 270–280.
- (18) Mazzini, A.; Cavatorta, P.; Iori, M.; Favilla, R.; Sartor, G. *Biophys. Chem.* **1992**, *42*, 101–109.
- (19) Ludescher, R. D.; Peting, L.; Hudson, S.; Hudson, B. *Biophys. Chem.* **1987**, *28*, 59–75.
- (20) Das, T. K.; Mazumdar, S. *Biophys. Chem.* **2000**, *86*, 15–28.
- (21) Bernhard, S. A.; Lee, B. A.; Tashjian, Z. H. *J. Mol. Biol.* **1966**, *18*, 405–420.
- (22) Dexter, D. L. *J. Chem. Phys.* **1953**, *21*, 836–850.
- (23) Dow, J. D. *Phys. Rev.* **1968**, *174*, 963–976.
- (24) Maiti, N. C.; Krishna, M. M. G.; Britto, P. J.; Periasamy, N. *J. Phys. Chem. B* **1997**, *101*, 11051–11060.
- (25) Smith, R. N.; Hansch, C. *Biochemistry* **1973**, *12*, 4924–4937.
- (26) McClure, W. O.; Edelman, G. M. *Biochemistry* **1967**, *6*, 559–566.
- (27) Johnson, J. D.; El-Bayoumi, M. A.; Weber, L. D.; Tulinsky, A. *Biochemistry* **1979**, *18*, 1292–1296.
- (28) Sigler, P. B.; Blow, D. M.; Matthews, B. W.; Henderson, R. *J. Mol. Biol.* **1968**, *35*, 143–164.